

Shell-model description of the beta decay of the $N=21$ isotones ^{35}Si and ^{36}P

E. K. Warburton

Brookhaven National Laboratory, Upton, New York 11973

J. A. Becker

Lawrence Livermore National Laboratory, Livermore, California 94550

(Received 16 December 1986)

The nuclear structure of the $N=21$ isotones ^{35}Si and ^{36}P and the $N=20$ isotones ^{35}P and ^{36}S is considered in the spherical nuclear shell model with the SDPF interaction. Beta and gamma decay as well as energy spectra are calculated. Results are compared to recent data on $^{36}\text{P}(\beta^-)^{36}\text{S}$ and $^{35}\text{Si}(\beta^-)^{35}\text{P}$. Unique and nonunique first-forbidden beta decay are considered as well as allowed (Gamow-Teller) decay. The predictions give a good description of the observed features of the four nuclei; in particular, the predicted beta decay rates are in agreement with experiment.

I. INTRODUCTION

Quite recently there has been a tremendous surge in the quality and quantity of experimental data on the beta decay of exotic light nuclei. Most impressive are the beta-gamma spectroscopy results from the GANIL intermediate energy heavy-ion facility.^{1,2} As a consequence of this activity, results for a large number of decaying neutron-rich nuclei which are available have not been explained by or even compared to nuclear structure calculations.

A nuclear spherical shell-model interaction, SDPF, was recently developed³ to describe those nuclear levels in the $A \simeq 35-43$ region for which the nucleons occupy more than one unfilled major shell. The model space for the SDPF interaction is the seven ($2s, 1d, 1f, 2p$) orbits. It is intended primarily for levels with 0-4 nucleons in the (fp) shell. As such, it is well suited to a description of allowed Gamow-Teller (GT) beta decay or first-forbidden beta decay in this mass region. And, in fact, it has already been applied to the beta decays of ^{35}P , ^{37}S , ^{38}S , and ^{38}Cl with considerable success.³

In this report we apply the SDPF interaction to the β^- decay of ^{35}Si and ^{36}P ; both nuclei are $N=21$ isotones and thus suited to the SDPF interaction and model space. The experimental results reported² for these decays are composed of lists of observed γ -ray energies and intensities. Thus, a part of the comparison of experiment and theory consists of the construction of decay schemes. In this, the shell-model predictions are used to some extent. For this reason, there is some correlation between the suggested decay schemes and the predicted ones, and the resulting decay schemes are somewhat model dependent.

We consider states composed of either 0 or 1 active particles in the fp shell and the rest in the (s, d) shell. Our predictions include energy spectra and allowed and first-forbidden (unique and nonunique) beta and gamma decay. We start with a brief description of the SDPF interaction and the beta- and gamma-decay calculations (Sec. II). The results for $^{36}\text{P}(\beta^-)^{36}\text{S}$ and $^{35}\text{Si}(\beta^-)^{35}\text{P}$ are presented in Secs. III and IV, respectively.

II. THE CALCULATION

A. The SDPF interaction

The SDPF interaction, described in detail in Ref. 3, consists of an inert ^{16}O core, the Wildenthal^{4,5} USD interaction for the (sd) shell, a modified Millener-Kurath⁶ (sd) to (fp) cross-shell interaction, and a modified van Hees-Glaudemans⁷ interaction for the (fp) shell. The modifications described in Ref. 3 were made to give better agreement with selected levels in $A=40-42$, while the $f_{7/2}, f_{5/2}, p_{3/2}, p_{1/2}$ single particle energies (SPE's) were adjusted to give agreement with the low-lying spectrum of ^{41}Ca . The computation in this and the previous work was carried out with the shell-model code OXBASH,⁸ which is formulated in the m scheme but utilizes projected basis vectors which have good J and T . Our calculations will be performed in the model spaces $(sd)^{A-16-n}(fp)^n$, with $n=0$ or 1. We shall refer to these spaces as $n\hbar\omega$ excitations. A small modification of the single-particle energies used in Ref. 3 was made, namely all four (fp) SPE's were raised by a further 279 keV. With this change the experimental ^{40}Ca binding energy becomes a reference point rather than the value calculated by the USD interaction, as was discussed in Ref. 3. Estimating the Coulomb-subtracted ^{40}Ca binding energy ($E_{B\text{corr}}$) from that of ^{39}Ca as given by Wildenthal⁵ results in the above-mentioned change of 279 keV in the single-particle energies for the (fp) shell. Note that this change does not affect wave functions calculated within a pure $n\hbar\omega$ model space.

B. Beta and gamma decay

Our procedures for calculating the decay half-lives, $\log ft$ values, and branching ratios follow closely the methods described by Wildenthal, Curtin, and Brown⁹ and applied by them to the beta decay of neutron-rich sd -shell nuclei. In particular, the beta-decay GT transition strength, $B_k(\text{GT})$, was calculated for all energetically accessible final states, k . This was found to demand ~ 100

final states of each of three of the allowed final spins, i.e., $J_f = J_i, J_i \pm 1$. The phase-space factor f was calculated using the Wilkinson-Macefield¹⁰ parametrization and for each state k the half-life, t_k , was calculated from

$$t_k = 6166 / [f \cdot B(\text{GT})]_k . \quad (1)$$

The total half-life for allowed decays is then obtained from

$$1/t = \sum_k (1/t_k) . \quad (2)$$

We use the effective Gamow-Teller operator described in Ref. 3 and based on the “final fit” sd -shell value of Brown and Wildenthal.¹¹ The resulting $B(\text{GT})$ values are $\sim 60\%$ of the $B(\text{GT})$ values obtained using the free nuclear Gamow-Teller operator. Thus, half-lives corresponding to the free nucleon GT operators would be $\sim 60\%$ of those presented here. Electromagnetic matrix elements are evaluated with harmonic oscillator radial wave functions, utilizing a length parameter b of $(41.467/\hbar\omega)^{1/2}$ fm with $\hbar\omega = 45A^{-1/3} - 25A^{-2/3}$ MeV. Magnetic transitions use the free-nucleon g factor, and $E2$ and $E3$ transitions are calculated with $e_p = 1.5e$, $e_n = 0.5e$.

We also consider first-forbidden beta decay, but to low-lying states only. In general, there are eight matrix elements contributing to a first-forbidden decay, so that a unique separation of the phase space and these matrix elements cannot be made. We start from $ft = 6166$ s for first-forbidden decays and the calculation includes combining the matrix elements with the appropriate phase-space and kinematical factors to give f . The procedures used for calculating unique first forbidden decays were described in Ref. 3. The shell-model space used is not adequate to give a good description of these decays,^{3,12} because we did not include ground-state correlations from $(n+2, \dots)\hbar\omega$ configurations in the final state. However, the effects of truncation of the final state to $n\hbar\omega$ only have been shown to result in an overestimation of the unique first-forbidden rate which is quite state independent. Thus, a reasonable estimate of the rate can be obtained by applying a “universal” correction factor to the shell-model prediction. We use a reduction factor of 4.2.

The capacity to calculate nonunique first-forbidden matrix elements was recently formulated for use with OXBASH (Ref. 13). The methods used are those of Millener and Warburton.¹⁴ The rank-0 contribution usually dominates $J \rightarrow J$ decays and is sensitive to the form of the radial wave functions. As in nuclei near $A \sim 16$ (Ref. 14), Woods-Saxon radial wave functions were used for these calculations. In the $A \sim 40$ region this gives a $\sim 30\%$ decrease in the rank-0 rate as compared to calculation with the harmonic oscillator radial form. We also include the expected meson exchange enhancement of the relativistic rank-0 matrix element. This enhancement is taken as 40%.¹⁴ The estimates for first-forbidden decay rates are less reliable than the Gamow-Teller predictions. However, we find that the contribution from first-forbidden decay is all but negligible for ^{35}Si and ^{36}P decay, so that further refinement is not necessary at this time.

III. $^{36}\text{P}(\beta^-)^{36}\text{S}$

A. The energy spectra

Relevant SDPF predicted and experimental binding energies for ^{35}Si , ^{35}P , ^{36}P , and ^{36}S are collected in Table I. The predicted and experimental binding energies of the lowest-lying $1\hbar\omega$ state is given for each nucleus. In addition, binding energies of the lowest-lying $0\hbar\omega$ state are given for ^{35}P and ^{36}S . These binding energies, $E_{B\text{corr}}$, do not include the Coulomb energy. The Coulomb-corrected experimental values for the $0\hbar\omega$ ground states of ^{35}P and ^{36}S were evaluated by Wildenthal.⁵ The predicted values for these two states are the “USD” predictions of Wildenthal.⁵ We consider the $1\hbar\omega$ states of ^{36}P and ^{36}S here and those of ^{35}Si and ^{35}P in the next section (Sec. III).

To obtain the Coulomb-corrected experimental binding energy, $E_{B\text{corr}}$, for the ^{36}S 3_1^- level we add the known¹⁵ experimental excitation energy of 4193 keV, while for ^{36}P we use the procedure of Wildenthal, Curtin, and Brown⁹ to estimate a Coulomb correction—including the $^1\text{H} - n$ mass difference—of 5069 keV to the measured $Q(\beta^-)$ for $^{36}\text{P}(\beta^-)^{36}\text{S}$ of 10413(13) keV. This latter value results from a weighted mean of two recent ^{36}P mass measurements^{16,17} and the assumption (see below) that the ground state of ^{36}P has $J^\pi = 4^-$. With this assumption, the SDPF overbinds ^{36}P by 530 keV.

Our predicted energy spectrum for ^{36}P has three levels below 1300 keV with $[J^\pi, E_x(\text{keV})]$ values of $(4^-, 0)$, $(3^-, 166)$, $(2^-, 602)$. Energy levels have been reported in ^{36}P at 252(10) keV (Ref. 16) and 450(22) keV (Ref. 17) from heavy-ion transfer reactions. The ^{36}Si β^- decay results of Ref. 2 suggest levels at 250.3(4) and 425.0(5) keV in agreement with the transfer results. These energies are in satisfactory accord with our predictions.

The ^{36}S energy spectra generated by the USD interaction ($0\hbar\omega$ levels; $\pi = +$) and the SDPF interaction ($1\hbar\omega$ levels; $\pi = -$) is compared to experiment in Fig. 1. Results of the present analysis of the $^{36}\text{P}(\beta^-)^{36}\text{S}$ reaction, discussed in the next subsection, are included in the experimental spectrum. Even parity states arising from $>0\hbar\omega$ excitations were identified by comparison to calculations

TABLE I. Experimental and predicted Coulomb corrected binding energies, $E_{B\text{corr}}$, for states of ^{35}Si , ^{35}P , ^{36}P , and ^{36}S . The difference (experiment – predicted) is also given.

Nucleus	State J^π	$E_{B\text{corr}}$ (MeV)		Diff. (MeV)
		Expt.	Pred.	
^{35}Si	$\frac{7}{2}^-$	–185.289	–185.845	0.556
^{35}P	$\frac{1}{2}^+$	–200.414	–200.660	0.246
^{35}P	$\frac{7}{2}^-$	–196.313	–196.606	0.293
^{36}P	4^-	–204.074	–204.604	0.530
^{36}S	0^+	–219.556	–219.533	–0.023
^{36}S	3^-	–215.363	–215.065	–0.298

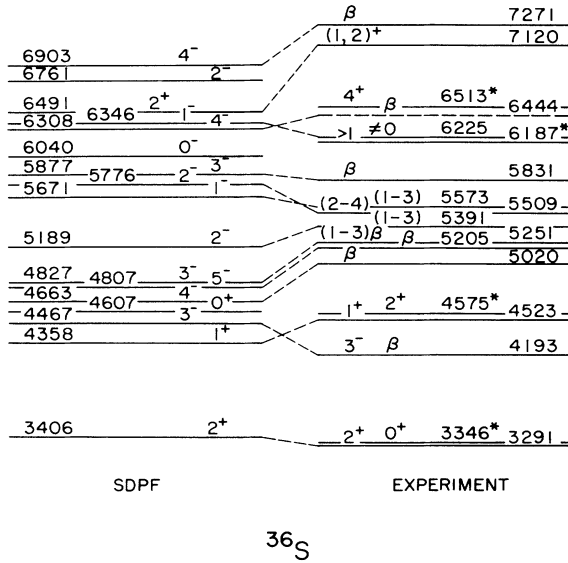


FIG. 1. The energy spectrum of ^{36}S . Note that the 0^+ ground state is omitted and the energy scale correspondingly suppressed. The excitation energies and J^π assignments of the experimental levels are from Ref. 15 and, if labeled by β , from Sec. III B. The SDPF calculation includes even-parity ($0\hbar\omega$) states from the USD interaction as well as odd-parity ($1\hbar\omega$) states. Our suggested correspondence of the predicted and calculated levels is indicated by dashed lines. Even-parity intruder ($>0\hbar\omega$) states are labeled by asterisks.

in a full $(d_{3/2}f_{7/2})^4$ model space using the WDF interaction¹⁸ and in a $[(s_{1/2}d_{3/2})^{8-n}(f_{7/2}p_{3/2})^n]$; $n=0,2,4$ model space using the van der Poel interaction.^{19,20} These states are outside our model space and are marked by asterisks in Fig. 1. Three of the four intruder states have been assigned definite J^π values. We identify the 6187-keV level with the second 2^+ intruder state.

The matching of the experimental and theoretical spectra is quite satisfactory. There appear to be missing experimental levels corresponding to the predicted 0^+ state at 4607 keV and the 0^- state at 6040 keV. Other than that, all theoretical states appear to have a reasonable experimental counterpart; i.e., one consistent with its known properties.

B. The β^- decay scheme

1. The experimental decay scheme

Guided by our SDPF predictions, we have constructed the $^{36}\text{P}(\beta^-)^{36}\text{S}$ decay scheme of Fig. 2 from the list of γ -ray energies and intensities of Ref. 2. All 22 γ rays listed in Ref. 2 are utilized; however, we interpret an entry of 3681.5 keV as the one-escape peak of a 4193-keV transition. The experimental γ -ray branching ratios shown in Fig. 2 result from the intensities of Ref. 2. We now turn to a comparison of the suggested decay scheme to our SDPF predictions.

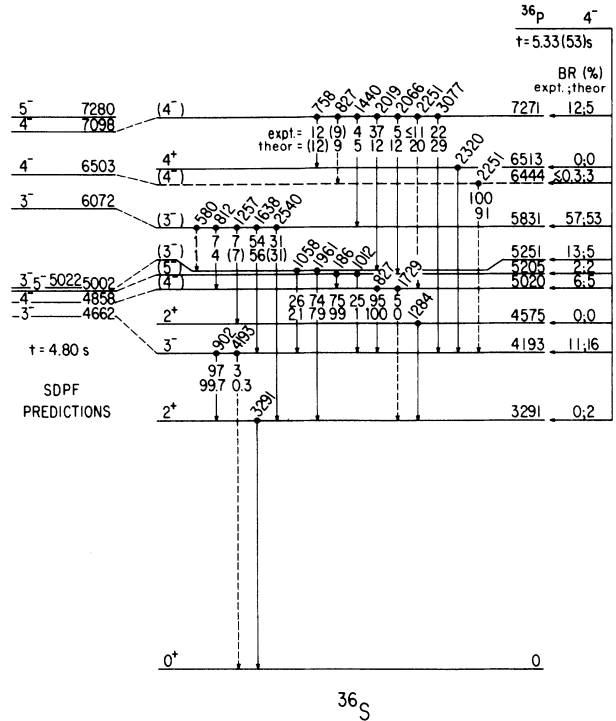


FIG. 2. The beta decay of ^{36}P . The SDPF predicted excitation energies to the left have been raised by 195 keV as in the β -decay calculation. The γ -ray energies are indicated in keV above the levels from which they originate. Gamma-ray branching ratios (in %) are given below the levels: the top numbers are experimental (Ref. 2) and the bottom are the SDPF predictions, as discussed in the text. Numbers in parentheses are assumed. The experimental and theoretical β branching ratios are indicated on the right.

Since the two lowest $1\hbar\omega$ states of ^{36}P are predicted to be a close-lying 4^- - 3^- doublet, we performed the beta-decay calculation for ^{36}P ground-state spins of both 4^- and 3^- . In these calculations, the relative excitation energies are taken from experiment whenever possible. Thus, we use the experimental value of $Q(\beta^-)$, 10 413(13) keV, and will place the ^{36}S 3_1^- level at 4193 keV (Ref. 15). Initially, the $Q(\beta^-)$ values for decay to the other ^{36}S $1\hbar\omega$ levels were taken from the SDPF predictions. For a ^{36}P 4^- ground state this procedure produced a half-life $t=4.6$ sec—as compared to the experimental value of 5.33(53) s—and β^- branching ratios in reasonable accord with experiment. For a ^{36}P 3^- ground state, we obtain $t=2.1$ s, with the only two β^- branches greater than 10% going to 3_1^- (55%) and 4_1^- (14%). Thus we conclude that a J^π of 4^- for the ^{36}P ground state is clearly favored by the shell model (as well as by systematics) and we do not consider the 3^- alternative any further.

With the adoption of a 4^- assignment for ^{36}P , a comparison of the SDPF energy spectrum and β^- decay rates leads us to the suggested ^{36}S spin-parity assignments of Fig. 2. We assume these assignments and further adjust (individually) the $Q(\beta^-)$ for the lowest seven 3^- - 5^- lev-

TABLE II. SDPF description of $^{36}\text{P}(\beta^-)^{36}\text{S}$. The predicted half-life is 4.80 s.

J_n^π	$E_x(\text{SDPF})^a$ (keV)	$E_x(\text{expt})^a$ (keV)	$B(\text{GT})$ ($\times 10^3$)	$\log ft^b$	Branching ratio (%)
2_1^+	3406	3291		$f = 21$	1.6
3_1^-	4467	4193	10.61	5.76	15.6
2_2^+		4575		$f = 7.5 \times 10^{-3}$	6.4×10^{-4}
4_1^-	4663	5020	6.69	5.96	5.2
5_1^-	4807	5205	2.78	6.34	1.8
3_2^-	4827	5251	17.06	5.94	4.5
3_3^-	5877	5831	144.9	4.63	52.8
4_2^-	6308	6444	17.71	5.54	3.3
4_1^+		6513		$f = 2.8 \times 10^{-4}$	2.4×10^{-3}
3_4^-	6820		0.73	6.93	0.1
4_3^-	6903	7271	73.11	4.93	4.7
5_2^-	7084		61.00	5.01	3.9
3_5^-	7139		6.16	6.00	0.4
3_6^-	7420		10.11	5.79	0.4
4_4^-	7545		25.95	5.38	0.8
5_3^-	7592		0.94	6.82	0.0
5_4^-	7841		12.55	5.69	0.2
4_5^-	7960		243.3	4.40	3.7
Total					99.0

^aWhen listed, the $E_x(\text{expt})$ were used in the calculation of f . For the remaining levels f was calculated using $E_x(\text{SDPF}) + 195$ keV.

^bFor nonunique first-forbidden decays, comparison to experiment is made via $ft = 6166$ s.

els of ^{36}S to agree with them. With this identification, the SDPF overbinds these seven states by an average value of 195 keV, so that in the calculation of the half-life we raise all higher-lying ^{36}S 3^- , 4^- , and 5^- levels by this amount. (Note that the SDPF predictions of Fig. 2 are also raised by 195 keV.)

The first-forbidden decay to the 2_1^+ state at 3291 keV was calculated with a $0\hbar\omega$ basis for this ^{36}S state. Decays to the 2_2^+ state at 4575 keV and the 4_1^+ state at 6513 keV were estimated from $(0+2)\hbar\omega$ calculations for these states, which we have identified as intruders. These calculations were carried out in the severely truncated model space of $d_{3/2}f_{7/2}$, but again the overestimation of the rates due to this truncation is known^{3,12} to be largely state independent and is given in Ref. 12 as 7 ± 1 . A factor of 7 was applied.

The results are summarized in Table II. The predicted branching ratios are also given in Fig. 2, where they are compared to the experimental ones. It is more efficient to delay discussion of these results until after the γ -ray decays have been considered.

C. Gamma-ray decays in ^{36}S

The calculated results for the electromagnetic rates are collected in Table III. We calculated all possible $M1$, $M2$, $E1$, $E2$, and $E3$ transitions, but results for higher multipoles, i.e., $L > |J_i - J_f|$, are only given when they contribute significantly to the decay rate or are needed for a full comparison to experiment. The predicted γ -ray branching ratios are also included in Fig. 2. Note that de-

cays involving the intruder states at 4575 and 6513 keV are excluded from consideration. Comparing to experiment, there are several cases of discrepancies where we believe summing of γ -ray cascades is a major contributor to the observed intensity and thus to the discrepancy.²¹ These include the $4193 \rightarrow 0$, 1729 -keV $5020 \rightarrow 3291$, and 1012 -keV $5205 \rightarrow 4193$ transitions, which are all cases where a weak crossover intensity would be significantly altered by a small amount of summing of two cascade transitions.

It is well known that $E1$ decay rates between low-lying nuclear states are difficult to predict accurately. That is particularly true in the $A \sim 40$ region, where the dominant configurations of $1\hbar\omega$ states involve excitations of $d_{3/2}$ nucleons to the $f_{7/2}$ shell, i.e., a $d_{3/2} \leftrightarrow f_{7/2}$ $E1$ transition is forbidden. In addition, a full $1\hbar\omega$ basis for $E1$ decays to $(sd)^n$ states in ^{36}S and ^{35}P should include $(1p)^{-1}(sd)^{n+1}$ terms as well as terms from $(sd)^{n-1}(fp)$. We think the discrepancy in the decay modes of the 5831-keV level is most likely due to an overestimation of the $3_3^- \rightarrow 2_1^+$ $E1$ rate. To test this hypothesis, we compare the branching ratios of Table III (which are the full calculated values) with the results shown in Fig. 2 for the 5831-keV level decay. In Fig. 2 the $3_3^- \rightarrow 2_1^+$ decay branch is excluded from consideration by giving it the experimental value. Then the relative rates of the three remaining transitions are in reasonable accord with experiment.

Note that the 827- and 2251-keV transitions are placed twice in Fig. 2. This is done to provide a candidate for the predicted 4_2^- state. Since the calculated β^- branch to this state is only 3%, it is quite possible that the γ transitions involving the 4_2^- state have been overlooked. It is

TABLE III. Predicted electromagnetic decays of odd-parity ^{36}S states. The transition strength $B(\lambda)$ is in units of $\mu_N^2 \text{fm}^{2L-2}$ for ML transitions and $e^2 \text{fm}^{2L}$ for EL transitions. Numbers in square brackets are powers of 10.

E_i (keV)	Initial	J_n^π	Final	λ	$B(\lambda)^a$	E_γ (keV)	Γ_γ (meV)	Branching ratio (%)
3291	2_1^+		0_1^+	$E2$				100.0
4193	3_1^-		0_1^+	$E3$	9.21[+ 2]	4193	7.89[- 3]	0.3
			2_1^+	$E1$	3.14[- 3]	902	2.41[+ 0]	99.7
5020	4_1^-		2_1^+	$M2$	1.75[- 1]	1729	5.63[- 6]	0.0
			3_1^-	$M1$	1.50[- 1]	827	9.84[- 1]	100.0
5205	5_1^-		3_1^-	$E2$	1.06[- 1]	1012	0.91[- 4]	0.6
			4_1^-	$M1$	2.11[- 1]	186	1.57[- 2]	99.4
5252	3_2^-		0_1^+	$E3$	1.66[+ 2]	5251	6.86[- 3]	0.1
			2_1^+	$E1$	6.02[- 4]	1961	4.75[+ 0]	79.1
			3_1^-	$M1$	9.12[- 2]	1059	1.25[+ 0]	20.8
5831	3_3^-		0_1^+	$E3$	3.81[+ 2]	5831	3.29[- 2]	0.0
			2_1^+	$E1$	3.98[- 3]	2540	6.82[+ 1]	96.0
			3_1^-	$M1$	4.99[- 2]	1638	2.54[+ 0]	3.6
			4_1^-	$M1$	3.06[- 2]	811	1.89[- 1]	0.3
			3_2^-	$M1$	2.46[- 2]	579	5.53[- 2]	0.1
6444	4_2^-		3_1^-	$M1$	4.40[- 2]	2251	5.81[+ 0]	91.4
				$E2$	1.55[+ 1]		7.23[- 1]	
			4_1^-	$M1$	8.05[- 5]	1425	2.69[- 3]	0.0
			5_1^-	$M1$	1.29[- 3]	1239	2.84[- 2]	0.4
			3_2^-	$M1$	2.15[- 2]	1193	4.22[- 1]	5.9
			3_3^-	$M1$	5.97[- 2]	613	1.59[- 1]	2.2
7271	4_3^-		3_1^-	$M1$	7.27[- 2]	3077	2.45[+ 1]	32.7
			4_1^-	$M1$	1.09[- 1]	2251	1.44[+ 1]	23.1
				$E2$	2.61[+ 1]		2.90[+ 0]	
			5_1^-	$M1$	1.03[- 1]	2066	1.05[+ 1]	14.0
			3_2^-	$M1$	1.07[- 1]	2020	1.02[+ 1]	13.6
			3_3^-	$M1$	1.32[- 1]	1440	4.56[+ 0]	6.1
			4_2^-	$M1$	1.21[+ 0]	827	7.91[+ 0]	10.5
7280	5_2^-		4_1^-	$M1$	1.29[- 3]	2260	1.72[- 1]	10.4
			4_2^-	$M1$	1.58[- 2]	836	1.07[- 1]	6.5
			4_3^-	$M1$	1.78[- 1]	92	1.60[- 6]	0.0
			5_1^-	$M1$	1.32[- 2]	2075	1.37[+ 0]	83.1

^aFor ^{36}S , single-particle (Weisskopf units) values for the $B(\lambda)$ are 0.703, 7.061, 76.988, and 1.791 for $E1$, $E2$, $E3$, and $M1$ transitions, respectively.

also possible that the 6513-keV level is actually the 4_2^- state and not the 4_1^+ state. [The 4_1^+ state is known to lie at 6509(8) keV (Ref. 15).] Thus, the 6444-keV level is only a suggestion; it is included in Fig. 2 to remind us that the 4_2^- level is expected somewhere in the vicinity.

D. Summary of results

The SDPF prediction for the half-life of ^{36}P is in agreement with experiment. It is possible to construct a $^{36}\text{P}(\beta^-)^{36}\text{S}$ decay scheme which is in quite good agreement with the SDPF predictions for both β and γ decay. The construction of this decay scheme is, of necessity, model dependent and further experiments—not necessari-

ly $^{36}\text{P}(\beta^-)^{36}\text{S}$ —are desirable to establish a scheme independently of any model.

The predicted β branching ratios of Fig. 2 are 90% of the decays. The remaining 10% is calculated to feed 4^- and 5^- levels with $E_x > 7$ MeV almost entirely (see Table II). Thus the γ deexcitation of these levels would feed the levels shown in Fig. 2 and a reduction of the experimental branching ratios by a total of 10% is predicted. Even with the uncertainty of how this reduction is distributed, the agreement of the predicted and experimental β decays is impressive.

The prediction of γ -decay rates does not seem to be as impressive. There are some strong discrepancies. However, some of these may be due to experimental error or to

errors in the proposed decay scheme. Again, further experimental study is desirable.

IV. $^{35}\text{Si}(\beta^-)^{35}\text{P}$

A. The energy spectra

For the $^{35}\text{P } \frac{5}{2}^-$ and $\frac{7}{2}^-$ states, the J -matrix dimensions for the full SDPF space are 3734 and 3808, respectively, and the available computer memory was not adequate to diagonalize the matrices. Thus, the number of $d_{5/2}$ holes was limited to three (the maximum possible is six) which gave J -matrix dimensions of 2665 and 2689, respectively. The effect of this truncation was examined by comparing calculations for $J = \frac{1}{2}, \frac{3}{2}, \frac{9}{2}, \frac{17}{2}$, and $\frac{19}{2}$ performed in the full SDPF model space with similar calculations performed in the truncated space. We found the effect of the truncation was to raise the binding energies (in keV) of the yrast states of these levels by 50, 56, 42, 55, and 43, respectively. The binding energies of the $\frac{5}{2}^-$ and $\frac{7}{2}^-$ states from the truncated calculation were all lowered by 50 keV to compensate for this effect. The truncation eliminated 0.1%, 0.2%, 0.1%, 0.2%, and 0.1% of these yrast wave functions, respectively. The effect of the truncation on the $^{35}\text{Si}(\beta^-)^{35}\text{P}(\frac{9}{2}^-)$ decay was less than 2% in

the overall rate and less than ± 0.4 in the percentage branching ratio for individual decays. This effect is small compared to other uncertainties.

The SDPF predicts an unusually high density of low-lying $1\hbar\omega$ states in ^{35}P with nine states in the first MeV. As expected, the lowest-lying of these has $J^\pi = \frac{7}{2}^-$. The experimental $E_{B, \text{corr}}$ for the ^{35}P ground state is calculated to be -200.414 MeV from results listed by Wildenthal.⁵ The experimental $E_{B, \text{corr}}$ for the first $1\hbar\omega$ state follows from our present conclusion (see Sec. IV B) that the $\frac{7}{2}_1^-$ level of ^{35}P lies at 4101 keV. There were no known odd-parity levels of ^{35}P previous to the work of Ref. 2 (Refs. 15, 22, and 23). However, a level observed²³ at 4474(21) keV with unknown J^π and small spectroscopic strength in the $(d, ^3\text{He})$ reaction may very well be the same level as the 4494-keV level of Fig. 3 (see below). There are also no known excited states of ^{35}Si . The mass excess of ^{35}Si has been measured via the $^{36}\text{S}(^{14}\text{C}, ^{15}\text{O})^{35}\text{Si}$ reaction¹⁷ and the $^{36}\text{S}(^{13}\text{C}, ^{14}\text{O})^{35}\text{Si}$ reaction.²⁴ In both cases only one outgoing oxygen group was observed. Fifield *et al.*²⁴ present rather convincing arguments that this group should be identified with the $\frac{7}{2}_1^-$ state of ^{35}Si , which is predicted to be the ground state. (The SDPF predicts a $\frac{3}{2}^-$ first-excited state at 1282 keV.) If so, the weighted mean of the two mass measurements gives a mass excess $-14.361(55)$ keV and $Q(\beta^-) = 10.497(55)$ MeV for $^{35}\text{Si}(\beta^-)^{35}\text{P}$. Applying a Coulomb correction⁹ of 4628 keV to this result gives the experimental $E_{B, \text{corr}}$ listed in Table I for ^{35}Si . We see that the SDPF overbinds ^{35}Si by 556 keV.

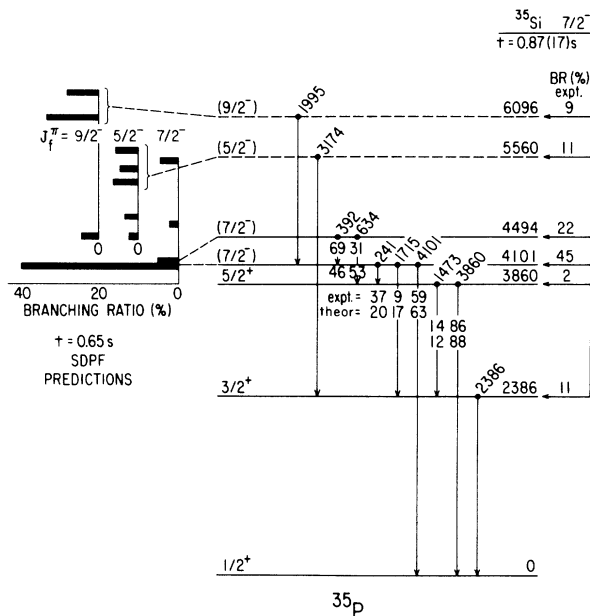


FIG. 3. The beta decay of ^{35}Si . The SDPF predicted excitation energies at the far left are placed relative to the assumed $\frac{7}{2}^-$ level at 4101 keV. The relative intensity of predicted β branches from Table IV is indicated in three separate graphs for the three possible ^{35}P final state spins. The experimental β -decay data, i.e., the total half-life and γ -ray energies and intensities, on the far right, are from Ref. 2. See the caption of Fig. 2 for more details.

B. The β^- decay scheme

The beta-decay calculation is summarized in Table IV and the suggested decay scheme is shown in Fig. 3. All γ transitions listed in Ref. 2 are included, except two, which are interpreted as one-escape peaks of the 3860- and 4101-keV levels.

Once again the predicted half-life, 0.65 s, is in good agreement with the experimental value, 0.87(17) s. The SDPF calculation suggests that there is a great deal of unreported flux into $1\hbar\omega$ levels. Our prediction from first-forbidden decay calculations is for essentially negligible flux into the known^{22,23} even-parity levels at 2386 and 3860 keV, whereas the two experimental β branches total 13%. Also, nine ^{35}P levels are predicted to have β branches to them of $> 3\%$ and only four are observed. From these facts, we conclude that the flux into the first two excited states is due to unobserved γ cascades from the γ decay of higher lying $\frac{5}{2}^-$ and $\frac{7}{2}^-$ states.

We see that it is possible to place the transitions so as to provide reasonable correspondences for the four observed β branches. The results quite clearly favor $\frac{7}{2}^-$ for the 4101-keV level. With this assignment we overpredict the binding of this level by 293 keV, a result in accord with the general trend for the SDPF interaction (see Table X of Ref. 3 as well as the results of Table I). We also note that the USD interaction overbinds the ^{35}P ground state by 246 keV—a rather larger amount than usual.⁵

TABLE IV. SDPF description of $^{35}\text{Si}(\beta^-)^{35}\text{P}$. The predicted half-life is 0.65 s.

J_n^π	$E_x(\text{SDPF})^a$ (keV)	$E_x(\text{expt})^a$ (keV)	$B(\text{GT})$ ($\times 10^3$)	$\log ft^b$	Branching ratio (%)
$\frac{3}{2}_1^+$	2630	2386		$f = 85$	0.9
$\frac{5}{2}_1^+$	4298	3857		$f = 0.08$	1.0×10^{-3}
$\frac{7}{2}_1^-$	4054	4101	180.70	4.53	40.5
$\frac{7}{2}_1^-$	4113	4494	21.86	5.45	4.7
$\frac{9}{2}_1^-$	4341		1.91	6.51	0.3
$\frac{5}{2}_2^-$	4410		10.53	5.77	1.8
$\frac{9}{2}_2^-$	4408		19.67	5.50	3.3
$\frac{7}{2}_3^-$	4614		15.81	5.59	2.3
$\frac{5}{2}_2^-$	4708		21.55	5.46	2.9
$\frac{5}{2}_3^-$	5166		63.05	4.99	5.8
$\frac{5}{2}_4^-$	5348		47.42	5.11	3.7
$\frac{7}{2}_4^-$	5453		56.20	5.04	4.0
$\frac{5}{2}_5^-$	5583		76.96	4.90	4.9
$\frac{7}{2}_5^-$	5791		13.46	5.66	0.7
$\frac{9}{2}_3^-$	5951		275.20	4.35	11.6
$\frac{5}{2}_6^-$	6056		23.79	5.41	1.0
$\frac{7}{2}_6^-$	6234		00.00	9.57	0
$\frac{9}{2}_4^-$	6279		237.00	4.41	7.0
$\frac{7}{2}_1^+$	7452			$f = 9 \times 10^{-3}$	1.0×10^{-4}
Total					95.4

^aWhen listed, the $E_x(\text{expt})$ were used in the calculation of f . For the remaining levels f was calculated for $E_x(\text{SDPF}) + 293$ keV.

^bFor nonunique first-forbidden decays, comparison to experiment is made via $ft = 6166$ s.

TABLE V. Predicted electromagnetic decays of ^{35}P states. The transition strength $B(\lambda)$ is in units of $\mu_N^2 \text{fm}^{2L-2}$ for ML transitions and $e^2 \text{fm}^{2L}$ for EL transitions. Numbers in square brackets are powers of 10.

E_i (keV)	$2J_n^\pi$ Initial	Final	λ	$B(\lambda)^a$	E_γ (keV)	Γ_γ (meV)	Branching ratio (%)		
2386	3_1^+	1_1^+	$M1$	2.43[−2]	2386	3.82[+0]	100		
			$E2$	2.45[+1]		1.53[+0]			
3860	5_1^+	1_1^+	$E2$	2.63[+1]	3860	1.82[+1]	88		
			3_1^+	$M1$	6.68[−2]	1473	2.47[+0]	12	
				$E2$	1.06[−3]		5.94[−6]		
4101	7_1^-	1_1^+	$E3$	1.04[+2]	4101	7.63[−4]	63		
			3_1^+	$M2$	1.58[+0]	1715	2.09[−4]	17	
				$E1$	1.62[−5]	241	2.38[−4]	20	
4494	7_2^-	1_1^+	$E3$	5.60[+2]	4494	7.79[−3]	0.5		
			3_1^+	$M2$	1.11[+1]	2107	4.11[−3]	0.3	
				5_1^+	$E1$	1.62[−3]	634	4.31[−1]	30
					$M1$	5.33[−1]	392	1.00[+0]	69

^aFor ^{35}P , single-particle (Weisskopf units) values for the $B(\lambda)$ are 0.690, 6.801, 72.770, 1.791, and 17.656 for $E1$, $E2$, $E3$, $M1$, and $M2$ transitions, respectively.

TABLE VI. ^{35}P $E1$ (top) and $M2$ (bottom) matrix elements predicted for ^{35}P using the SDPF interaction. The units are $e\text{ fm}$ for $E1$ and $\mu_N\text{ fm}$ for $M2$ decays. Numbers in square brackets are powers of 10.

J_A^π	J_B^π	n_B	1	2	n_A 3	4	5
$M(\lambda)$							
$\frac{5}{2}^-$	$\frac{3}{2}^+$	1	-8.352[-2] 7.212[-1]	8.297[-2] 2.995[-1]	1.258[-1] 2.410[-1]	1.015[-1] 1.814[-1]	-1.050[-1] 7.973[-2]
		2	-4.925[-2] 1.199[+0]	-5.607[-2] 9.960[-1]	-3.868[-2] 1.313[+0]	6.256[-2] 2.621[-1]	-5.380[-2] 1.636[+0]
$\frac{5}{2}^-$	$\frac{5}{2}^+$	1	-9.747[-3] 1.930[-1]	-1.810[-2] 8.456[-1]	5.137[-2] 8.656[-1]	8.367[-3] 1.494[+0]	-5.267[-2] 3.861[-1]
		2	-2.893[-2] 3.475[-1]	1.208[-2] 2.676[-1]	-2.078[-2] 7.156[-1]	9.190[-3] 1.221[-1]	3.444[-3] 3.091[-1]
$\frac{7}{2}^-$	$\frac{5}{2}^+$	1	1.138[-2] 4.830[-1]	-1.138[-1] 3.067[+0]	-1.049[-1] 4.643[-1]	-1.155[-1] 2.235[+0]	1.228[-1] 6.774[-1]
		2	-5.128[-2] 7.237[-1]	-5.909[-2] 2.033[+0]	1.440[-3] 2.673[-1]	5.547[-2] 2.002[+0]	-2.077[-2] 5.224[-2]
$\frac{9}{2}^-$	$\frac{5}{2}^+$	1	— 2.648[-1]	— 2.465[+0]	— 3.828[+0]	— 1.572[+0]	— 1.868[+0]
		2	— 3.040[-1]	— 1.605[+0]	— 1.469[+0]	— 1.635[+0]	— 1.342[+0]

C. Gamma-ray decays in ^{35}P

Calculated results for the γ decay of the lowest four states of Fig. 3 are given in Table V. Only results contributing significantly to these decay rates are listed. The predicted branching ratios are also included in Fig. 3,

where they are compared to the experimental results from Ref. 2. The agreement is impressively good, adding credence to the decay scheme proposed up to $E_x = 5\text{ MeV}$.

As is clear from Fig. 3, it is not possible to correlate the proposed 5560- and 6096-keV levels with any particular $1\hbar\omega$ model state. We list in Tables VI and VII predicted

TABLE VII. Predicted $M1$ (top) and $E2$ (bottom) matrix elements for ^{35}P $1\hbar\omega$ states obtained with the SDPF interaction. The units of $M(\lambda)$ are μ_N for $M1$ and $e\text{ fm}^2$ for $E2$ decays. Numbers in square brackets are powers of 10.

J_A^π	J_B^π	n_B	1	2	n_A 3	4	5
$M(\lambda)$							
$\frac{5}{2}^-$	$\frac{5}{2}^-$	1		-2.415[+0] 6.883[+0]	+2.327[-1] 1.418[+0]	+5.065[-1] 5.492[+0]	+1.158[-1] 3.891[-1]
		2			+6.271[-2] 5.981[+0]	-9.679[-1] 2.112[+0]	+2.081[-1] 7.536[-1]
		3				-2.840[-2] 1.435[+0]	-4.589[-1] 2.714[+0]
		4					+2.496[-1] 5.891[+0]
$\frac{7}{2}^-$	$\frac{5}{2}^-$	1	+2.139[-1] 2.173[+0]	-1.585[+0] 3.376[+0]	-1.400[+0] 5.198[-1]	+2.734[-1] 5.173[+0]	+3.963[-1] 5.092[+0]
		2	-1.693[+0] 2.679[+0]	-1.776[+0] 5.007[+0]	-1.442[+0] 1.031[+1]	-4.865[-1] 3.637[+0]	-5.463[-1] 1.021[+1]
		3	+2.236[-1] 5.193[+0]	-5.030[-1] 6.753[+0]	-1.127[-2] 3.421[+0]	-2.068[+0] 7.847[+0]	+9.361[-1] 3.993[+0]
		4	+4.175[-1] 2.027[+0]	+2.409[-1] 1.352[+0]	-1.977[+0] 2.926[-1]	-1.882[-1] 3.138[+0]	+9.682[-1] 2.156[+0]
		5	+4.863[-1] 1.298[+0]	+1.470[+0] 3.140[+0]	-1.329[+0] 1.258[+1]	-5.147[-1] 4.723[+0]	-1.187[+0] 2.480[+0]

TABLE VII. (Continued).

J_A^π	J_B	n_B	1	2	n_A 3	4	5
$M(\lambda)$							
$\frac{7}{2}^-$	$\frac{7}{2}^-$	1		-2.065[+ 0] 1.189[+ 0]	-5.264[- 1] 1.491[+ 0]	+ 6.157[- 2] 3.591[+ 0]	+ 4.330[- 1] 1.430[+ 0]
		2			-1.199[+ 0] 1.013[+ 0]	-1.433[+ 0] 1.287[- 1]	-2.024[- 1] 5.092[+ 0]
		3				+ 2.641[- 1] 1.601[+ 0]	-6.481[- 1] 3.368[+ 0]
		4					-8.261[- 2] 2.193[+ 0]
$\frac{9}{2}^-$	$\frac{7}{2}^-$	1	+ 5.394[- 1] 9.853[+ 0]	-1.073[+ 0] 1.031[+ 1]	+ 3.581[- 1] 8.151[+ 0]	-4.758[- 1] 1.089[+ 0]	+ 5.433[- 1] 6.241[+ 0]
		2	-2.306[+ 0] 1.867[+ 0]	-1.785[+ 0] 1.280[+ 1]	+ 6.894[- 1] 5.777[+ 0]	+ 3.198[- 1] 2.213[+ 0]	-3.647[- 1] 5.787[+ 0]
		3	-1.760[+ 0] 9.863[+ 0]	-5.809[- 1] 8.920[+ 0]	-5.154[- 1] 9.009[+ 0]	-2.304[- 1] 2.744[+ 0]	-1.573[- 1] 5.743[+ 0]
		4	-7.424[- 1] 9.151[+ 0]	-8.467[- 1] 3.112[+ 0]	+ 7.187[- 1] 2.906[+ 0]	-1.927[- 1] 1.120[+ 0]	+ 4.853[- 1] 3.028[+ 0]
		5	+ 6.793[- 1] 5.481[- 1]	+ 1.046[- 1] 4.386[+ 0]	-1.732[+ 0] 4.218[+ 0]	+ 1.602[- 1] 4.263[+ 0]	+ 1.316[- 1] 4.266[+ 0]
$\frac{9}{2}^-$	$\frac{9}{2}^-$	1		+ 1.148[+ 0] 4.021[- 1]	-7.344[- 1] 1.396[+ 1]	-1.216[+ 0] 2.165[+ 0]	+ 2.968[- 1] 4.593[+ 0]
		2			-4.051[- 1] 1.142[+ 0]	-3.677[- 1] 4.372[+ 0]	-6.357[- 2] 7.240[- 1]
		3				+ 4.790[- 1] 2.179[+ 0]	-5.612[- 1] 7.691[+ 0]
		4					+ 3.645[- 1] 1.657[+ 1]

electromagnetic matrix elements involving the first five ($n=1-5$) states of $J^\pi = \frac{5}{2}^-$, $\frac{7}{2}^-$, and $\frac{9}{2}^-$. The matrix element $M(\lambda)$ is defined by

$$|M(\lambda)|^2 = (2J_i + 1)B(\lambda). \quad (3)$$

The sign convention for $L+1, L$ admixtures is that of Rose and Brink.²⁵ These matrix elements should be of use in the event that $^{35}\text{Si}(\beta^-)^{35}\text{P}$ is studied with more sensitivity to weaker γ transitions.

V. SUMMARY

We have used the SDPF shell-model interaction to generate wave functions for $1\hbar\omega$ states of ^{36}P , ^{36}S , ^{35}Si , and ^{35}P and $0\hbar\omega$ states of ^{36}S and ^{35}P . Binding energies and β^-/γ decay rates were calculated. The results are in good accord with the known properties of these nuclei. In particular, the β^- decay rates of ^{36}P and ^{35}Si are in agreement with experiment² and the calculated γ -ray decay rates add credence to the proposed decay schemes. Re-

sults of SDPF predictions have now been presented here and in Ref. 3 for $1\hbar\omega$ states in the $N=21$ isotones ^{35}Si , ^{36}P , ^{37}S , and ^{38}Cl . Results for ^{39}Ar are in progress.²⁶ These are the first shell-model calculations reported in this nuclei utilizing the full SDPF model space. It was expected that this full SDPF model space would be needed in order to obtain a good description of allowed beta decay. But, of course, use of such a model space does not guarantee the effectiveness of the SDPF interaction. It is satisfying that results obtained to date with the SDPF interaction are in such good accord with experiment.

ACKNOWLEDGMENTS

We would like to thank J. P. Dufour and B. A. Brown for valuable discussions. This research was supported by the U. S. Department of Energy under Contracts No. DE-AC02-76CH00016 (Brookhaven National Laboratory) and No. W-7405-Eng-48 with the University of California (Lawrence Livermore National Laboratory).

- ¹M. Langevin, E. Quiniou, M. Bernas, J. Galin, J. C. Jacmart, F. Naulin, F. Pougheon, R. Anne, C. Détraz, D. Guerreau, D. Guillemaud-Mueller, and A. C. Mueller, *Phys. Lett.* **150B**, 71 (1985); D. Guillemaud-Mueller, A. C. Mueller, D. Guerreau, F. Pougheon, R. Anne, M. Bernas, J. Galin, J. C. Jacmart, M. Langevin, F. Naulin, E. Quiniou, and C. Détraz, *Z. Phys. A* **322**, 415 (1985).
- ²J. P. Dufour, R. Del Moral, A. Fleury, E. Hubert, D. Jean, M. S. Pravikoff, H. Delagrangé, H. Geissel, and K.-H. Schmidt, *Z. Phys. A* **324**, 487 (1986). It should be emphasized that this is a preliminary report and the data will almost certainly be revised somewhat before decay schemes are published.
- ³E. K. Warburton, D. E. Alburger, J. A. Becker, B. A. Brown, and S. Raman, *Phys. Rev. C* **34**, 1031 (1986).
- ⁴B. H. Wildenthal, *Prog. Part. Nucl. Phys.* **11**, 5 (1984).
- ⁵A comprehensive report of results of the USD interaction (Ref. 4) has not as yet been published. However, a summary of binding energies for $A = 17-39$ has been privately circulated by B. H. Wildenthal.
- ⁶D. J. Millener and D. Kurath, *Nucl. Phys.* **A255**, 315 (1975).
- ⁷A. G. M. van Hees and P. W. M. Glaudemans, *Z. Phys. A* **303**, 267 (1980).
- ⁸B. A. Brown, A. Etchegoyen, W. D. M. Rae, and N. S. Godwin, OXBASH, 1984 (unpublished).
- ⁹B. H. Wildenthal, M. S. Curtin, and B. A. Brown, *Phys. Rev. C* **28**, 1343 (1983).
- ¹⁰D. H. Wilkinson and B. E. F. Macefield, *Nucl. Phys.* **A232**, 58 (1974).
- ¹¹B. A. Brown and B. H. Wildenthal, *At. Data Nucl. Data Tables* **33**, 347 (1985).
- ¹²E. K. Warburton, G. T. Garvey, and I. S. Towner, *Ann. Phys. (N.Y.)* **57**, 174 (1970); I. S. Towner, E. K. Warburton, and G. T. Garvey, *ibid.* **66**, 674 (1971).
- ¹³E. K. Warburton, D. J. Millener, B. A. Brown, and J. A. Becker, *Bull. Am. Phys. Soc.* **31**, 1222 (1986).
- ¹⁴D. J. Millener and E. K. Warburton, in *Proceedings of the International Symposium on Nuclear Shell Models*, edited by M. Vallieres and B. H. Wildenthal (World-Scientific, Singapore, 1985), p. 365.
- ¹⁵P. M. Endt and C. van der Leun, *Nucl. Phys.* **A310**, 1 (1978).
- ¹⁶P. V. Drumm, L. K. Fifield, R. A. Bark, M. A. C. Hotchkis, and C. L. Woods, *Nucl. Phys.* **A441**, 95 (1985).
- ¹⁷W. A. Mayer, W. Henning, R. Holzworth, G. Korschinek, W. V. Mayer, G. Rosner, and H. J. Scheerer, *Z. Phys.* **A319**, 287 (1984).
- ¹⁸B. H. Wildenthal, private communication, see Ref. 3.
- ¹⁹G. J. L. Nooren and C. van der Leun, *Nucl. Phys.* **A423**, 197 (1984); G. J. L. Nooren, H. P. L. de Esch, and C. van der Leun, *ibid.* **A423**, 228 (1984).
- ²⁰Both of these interactions are more suited than ours to calculations in mixed $(n, n+2, \dots)$ $h\omega$ spaces. See Ref. 3 for a discussion of this point.
- ²¹The gamma-ray detector efficiency in the decay scheme studies of Ref. 2 was large enough to result in considerable summing contributions for weak crossover transitions. The remark in Ref. 2 limiting summing corrections to $< 10\%$ was intended to apply to the major branches only. J. P. Dufour, private communication.
- ²²C. E. Thorn, J. W. Olness, E. K. Warburton, and S. Raman, *Phys. Rev. C* **30**, 1442 (1984).
- ²³S. Khan, T. Kihm, K. T. Knöpfle, G. Maisle, V. Bechtold, and L. Friedrich, *Phys. Lett.* **156B**, 155 (1985).
- ²⁴L. K. Fifield, C. L. Woods, W. N. Catford, R. A. Bark, P. V. Drumm, and K. T. Keoghan, *Nucl. Phys.* **A453**, 497 (1986).
- ²⁵H. J. Rose and D. M. Brink, *Rev. Mod. Phys.* **39**, 306 (1967).
- ²⁶E. K. Warburton (unpublished).